

Characteristic Modes Extraction of Dielectric Bodies Using Pulse Functions

Sevda Özdemir^{*(1)}, Shang Xiang⁽²⁾, and Buon Kiong Lau⁽²⁾

(1) Department of Electrical and Electronics Engineering, Hacettepe University, Ankara, Turkey

(2) Electrical and Information Technology, Lund University, Lund, Sweden



Contents

- Theory of Electric Field Integral Equation (EFIE)
- Volume Integral Equation (VIE) Using Pulse Functions
- Theory of Characteristic Mode (TCM) Using Pulse Functions
- Numerical Examples and Results
- Conclusion

Theory of Electric Field Integral Equation

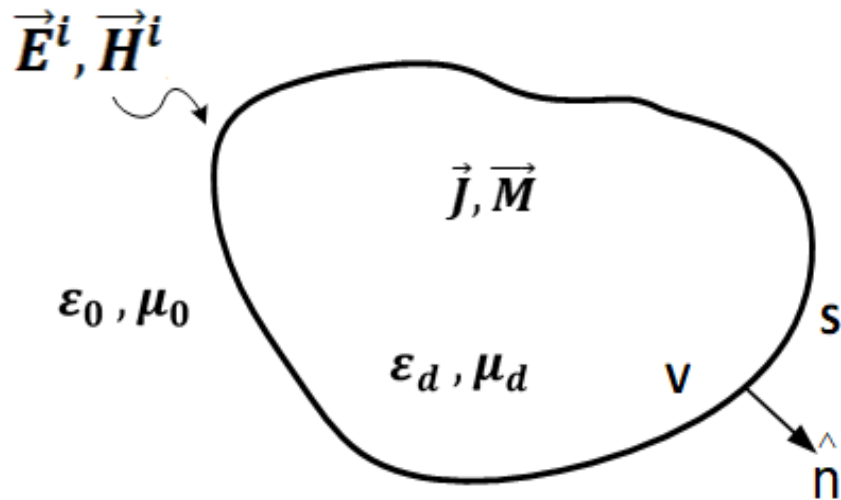


Figure 1: Scattering problem illuminated by sources \mathbf{E}^i and \mathbf{H}^i ($\epsilon_d \neq 1, \mu_d = 1$)

Electric field integral equation (EFIE) is written in terms of the electric current density $\mathbf{J}(\mathbf{r})$ for an inhomogeneous isotropic dielectric body:

$$\mathbf{E}(\mathbf{r}) = \mathbf{E}^i(\mathbf{r}) + \mathbf{E}^s(\mathbf{r})$$

$$\mathbf{E}^s(\mathbf{r}) = -\frac{j\omega\mu_0}{4\pi} \int_{V'} \mathbf{J}(\mathbf{r}') G dv' - \frac{\nabla}{j\omega 4\pi\epsilon_0} \oint_{S'} \hat{\mathbf{n}} \cdot \mathbf{J}(\mathbf{r}') G ds'$$

$\mathbf{E}(\mathbf{r})$: total electric field

$\mathbf{E}^s(\mathbf{r})$: scattered electric field

$\mathbf{E}^i(\mathbf{r})$: incident electric field

$\mathbf{J}(\mathbf{r})$: electric current density

$G = \exp(-jkR)/R$

$R = |\mathbf{r} - \mathbf{r}'|$, distance between observation & source points

Volume Integral Equation Using Pulse Functions

- The dielectric region is divided into tetrahedral cells
- The electric current density is expanded using pulse functions:

$$\mathbf{J}(\mathbf{r}) = \sum_{i=1}^M \hat{\mathbf{x}} J_i^x \mathcal{P}_i(\mathbf{r}) + \hat{\mathbf{y}} J_i^y \mathcal{P}_i(\mathbf{r}) + \hat{\mathbf{z}} J_i^z \mathcal{P}_i(\mathbf{r})$$

M : number of unknown

J_x^i, J_y^i and J_z^i : x, y, z components of electric current density

$\mathcal{P}_i(\mathbf{r})$: pulse basis function

- After applying the point matching technique, the linear equations for Method of Moments (MoM) matrix is obtained as:

$$\begin{bmatrix} Z(\mathbf{J}_{ij}^{xx}) & Z(\mathbf{J}_{ij}^{xy}) & Z(\mathbf{J}_{ij}^{xz}) \\ Z(\mathbf{J}_{ij}^{yx}) & Z(\mathbf{J}_{ij}^{yy}) & Z(\mathbf{J}_{ij}^{yz}) \\ Z(\mathbf{J}_{ij}^{zx}) & Z(\mathbf{J}_{ij}^{zy}) & Z(\mathbf{J}_{ij}^{zz}) \end{bmatrix} \begin{bmatrix} J_x \\ J_y \\ J_z \end{bmatrix} = \begin{bmatrix} E_x^{inc} \\ E_y^{inc} \\ E_z^{inc} \end{bmatrix}$$

TCM Using Pulse Functions

- EFIE due to impressed current $\mathbf{J}(\mathbf{r})$:

$$\left. \begin{aligned} Z_v(\mathbf{J}) + (j\omega\Delta\varepsilon)^{-1}\mathbf{J} &= \mathbf{E}^i \\ Z &= Z_V + (j\omega\Delta\varepsilon)^{-1} \\ \Delta\varepsilon &= \varepsilon - \varepsilon_0 \end{aligned} \right\} \rightarrow Z(\mathbf{J}) = \mathbf{E}^i$$

- The eigenvalue equation using TCM is defined as:

$$X \cdot J_n = \lambda_n R \cdot J_n$$

R : real part of impedance operator Z

X : imaginary part of impedance operator Z

λ_n : characteristic values of the generalized eigenvalue problem

J_n : real valued currents of the generalized eigenvalue problem

- The induced total current J under external excitations with the modal weighting coefficient V_n^i :

$$J = \sum_{n=1}^M \frac{V_n^i J_n}{1 + j\lambda_n} \quad , \quad V_n^i = \langle J_n, E^i \rangle = \int_{V'} J_n \cdot E^i d\tau'$$

- The complex power radiated by the induced current \mathbf{J} in the dielectric body illuminated by the incident field \mathbf{E}^i is given by:

$$P = \langle \mathbf{J}^*, \mathbf{ZJ} \rangle = \langle \mathbf{J}^*, \mathbf{RJ} \rangle + j \langle \mathbf{J}^*, \mathbf{XJ} \rangle$$

- For the n -th CM, the real part of complex power is:

$$\langle \mathbf{J}_n^*, \mathbf{RJ}_n \rangle = \text{Re} \langle \mathbf{J}_n^*, \mathbf{ZJ}_n \rangle = \text{Re}(P)$$

- For the n -th CM, the imaginary part of $\langle \mathbf{J}_n^*, \mathbf{ZJ}_n \rangle$ is:

$$\langle \mathbf{J}_n^*, \mathbf{XJ}_n \rangle = \text{Im} \langle \mathbf{J}_n^*, \mathbf{ZJ}_n \rangle - \frac{1}{\omega} \int_{V'} \mathbf{J}_n^* \cdot (\Delta \boldsymbol{\epsilon})^{-1} \mathbf{J}_n \, dv'$$

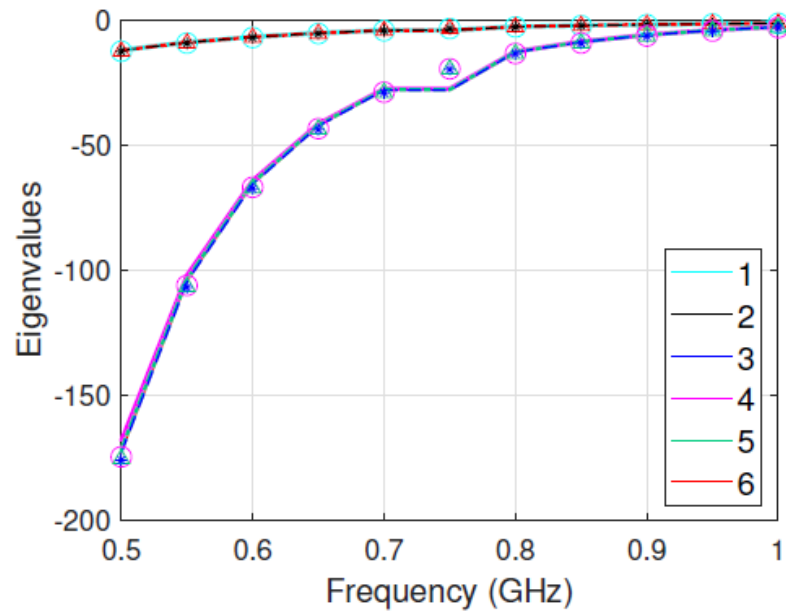
Numerical Examples and Results

- MoM solution of VIE is compared with Altair[®] FEKO simulation program which uses SWG basis functions
- The incident angles of the plane wave are $\theta^i = 0^\circ$ and $\varphi^i = 0^\circ$
- The power ratios (PRs) of the real and imaginary parts of $\langle \mathbf{J}^*, \mathbf{ZJ} \rangle$ for the proposed (pulse) and SWG methods can be calculated as follows:

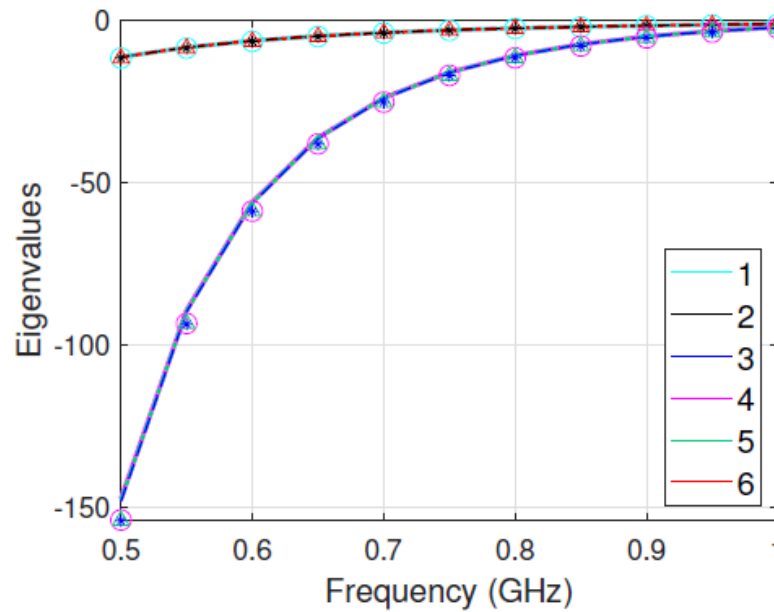
$$PR_{real} = \frac{Re\langle \mathbf{J}^*, \mathbf{ZJ} \rangle_{pulse}}{Re\langle \mathbf{J}^*, \mathbf{ZJ} \rangle_{SWG}}, \quad PR_{imag} = \frac{Im\langle \mathbf{J}^*, \mathbf{ZJ} \rangle_{pulse}}{Im\langle \mathbf{J}^*, \mathbf{ZJ} \rangle_{SWG}}$$

- A convergence study of \mathbf{J} is performed using the error norm between induced current under external excitations of CMA and SWG methods:

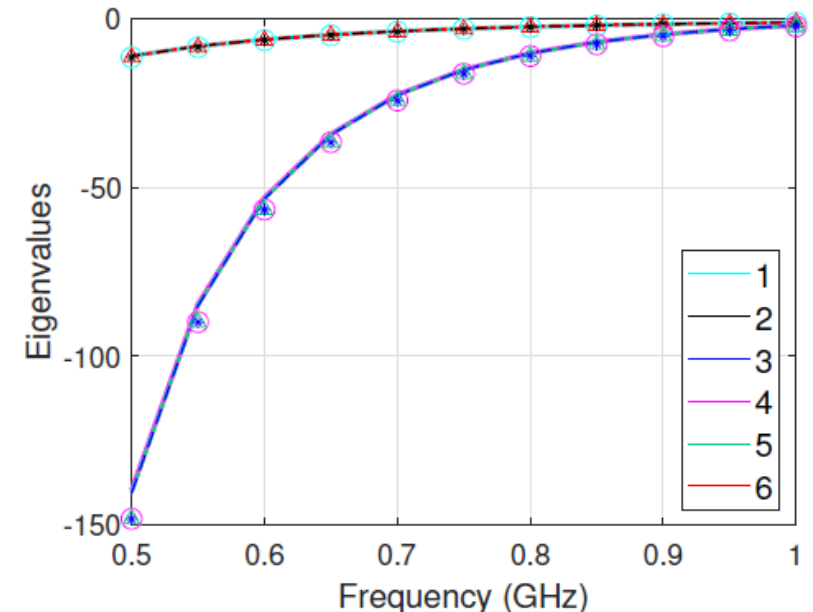
$$Error(\mathbf{J}) = \frac{\|\mathbf{J}_{pulse} - \mathbf{J}_{SWG}\|}{\|\mathbf{J}_{SWG}\|}$$



(a)



(b)



(c)

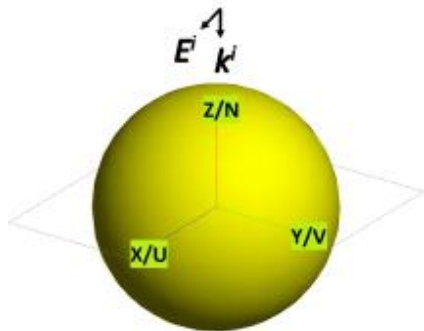
Figure 2: Eigenvalues of the first 6 CMs of a $0.2\lambda_0$ sphere for different number of meshes, $\epsilon_r = 4$. The coloured shapes ($\circ, \Delta, *$) are for FEKO[®]'s CM results.

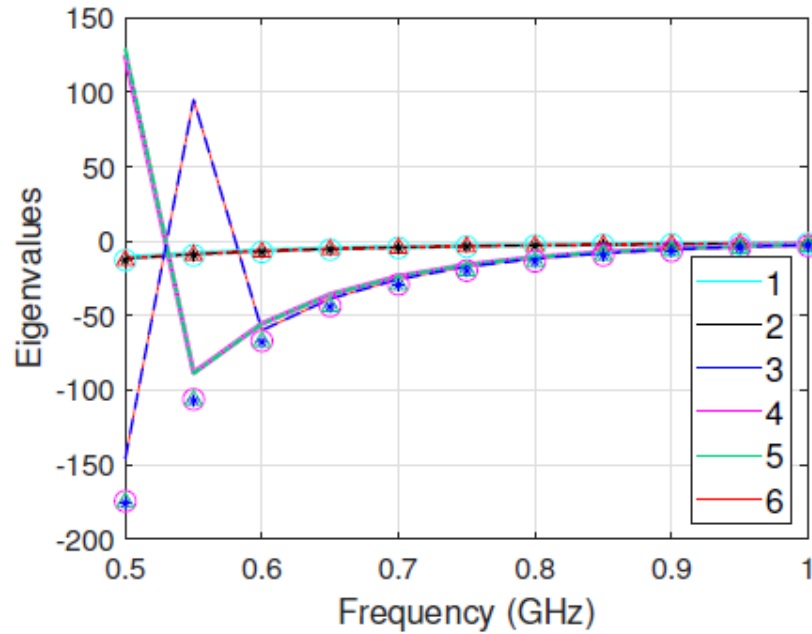
(a) $TEL = \lambda_{eff}/5$, 307 tetrahedrons,

(b) $TEL = \lambda_{eff}/7.5$, 1160 tetrahedrons,

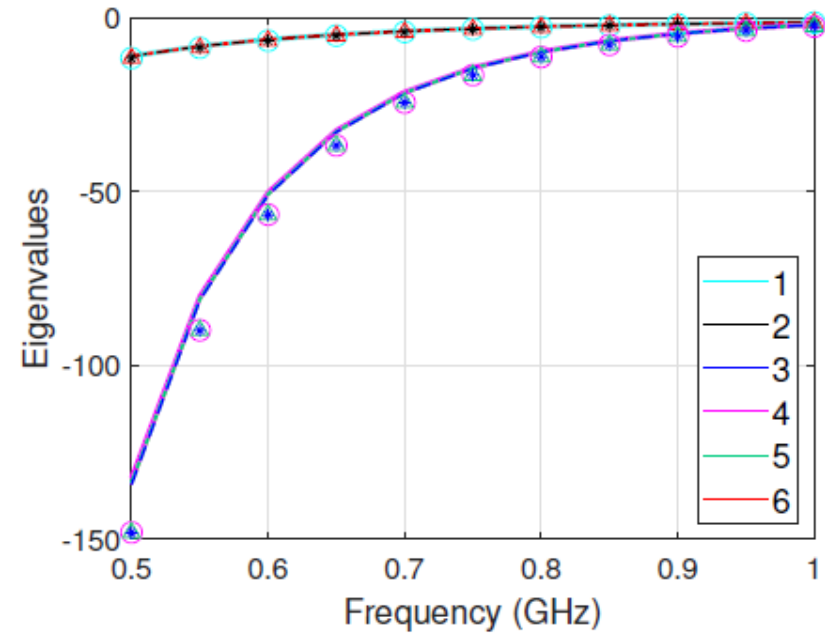
(c) $TEL = \lambda_{eff}/10$, 2772 tetrahedrons.

NB: a, b, c \rightarrow meshed using FEKO, TEL: tetrahedron edge lengths, $\lambda_{eff} = \lambda_0 / \sqrt{\epsilon_{eff}}$





(d)



(e)

Figure 2 (cont'd): Eigenvalues of the first 6 CMs of a $0.2\lambda_0$ sphere for different number of meshes, $\epsilon_r = 4$ (The coloured shapes ($\circ, \Delta, *$) are for FEKO[®]'s CM results.

(d) $TEL = \lambda_{eff}/5$, 302 tetrahedrons,

(e) $TEL = \lambda_{eff}/10$, 3398 tetrahedrons.

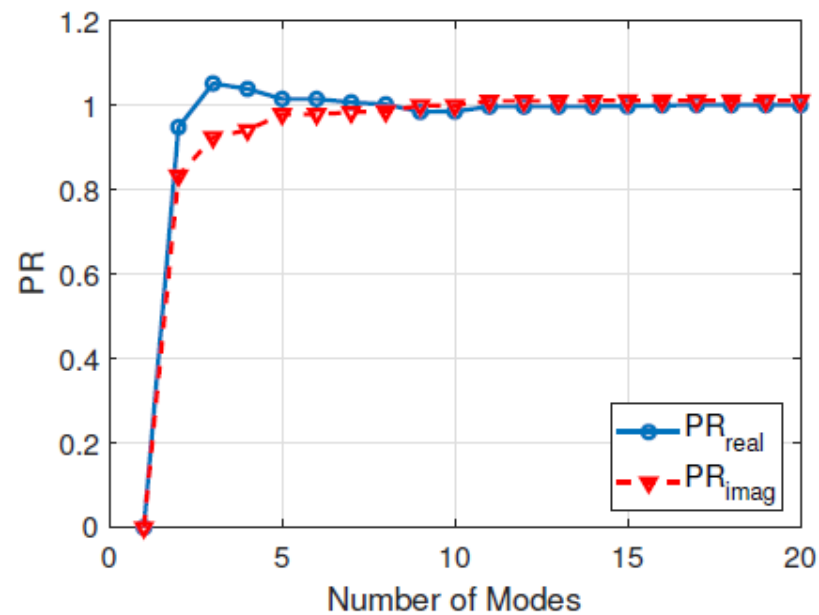
NB: d,e→meshed using FEMLAB , TEL: tetrahedron edge lengths, $\lambda_{eff} = \lambda_0 / \sqrt{\epsilon_{eff}}$

Table 1. The eigenvalue of first 6 the CMs for the $0.2\lambda_0$ sphere for different number of meshes at $f_0 = 1$ GHz

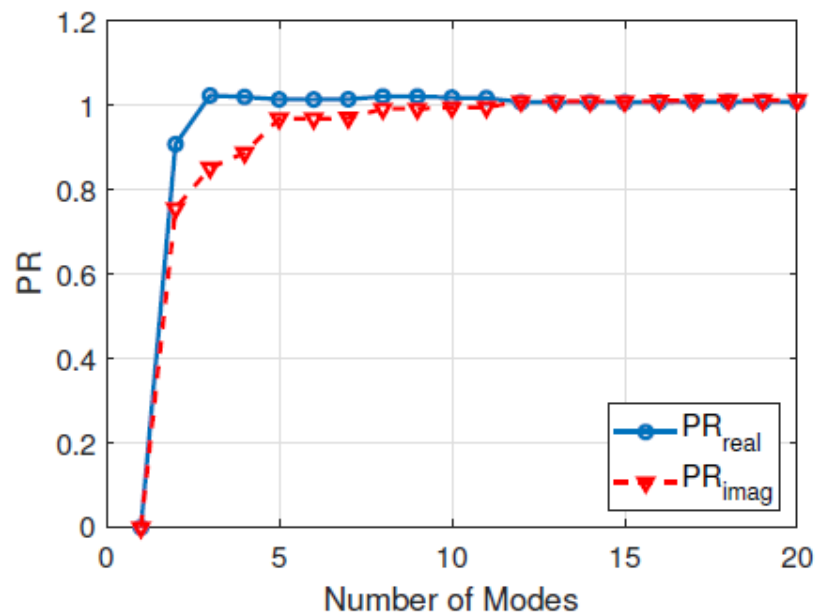
CM #	$\lambda_{eff}/5$	$\lambda_{eff}/10$	$\lambda_{eff}/12.5$
1	-1.330	-1.293	-1.291
2	-1.332	-1.297	-1.293
3	-1.337	-1.299	-1.295
4	-2.355	-2.142	-2.128
5	-2.370	-2.167	-2.139
6	-2.388	-2.172	-2.157

NB: Meshing with Altair FEKO[®], solved using pulse functions.

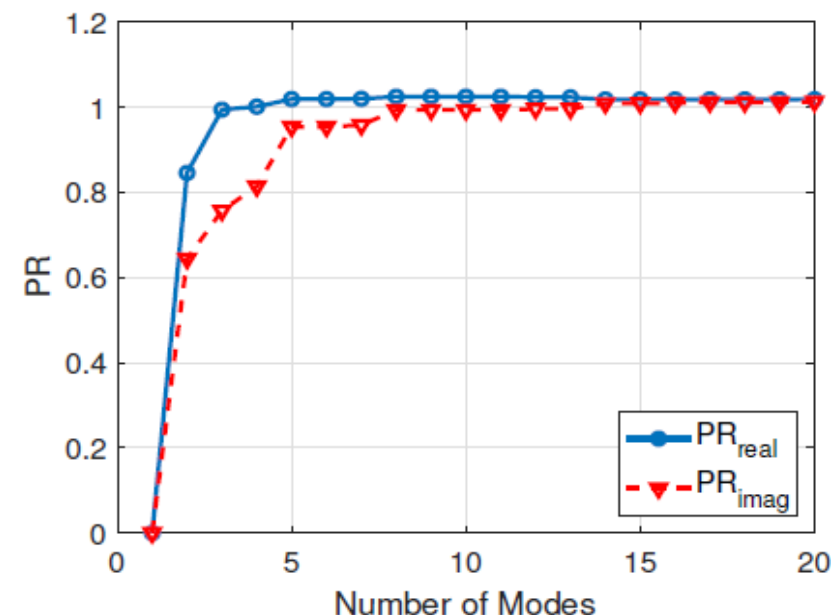
- As the number of meshes increases, the characteristic eigenvalues appear to converge well for the first 6 CMs when the TEL is $\lambda_{eff}/10$
- Different meshes generated by Altair FEKO[®] and FEMLAB[®] change the CM results, especially for the larger (negative) eigenvalues



(a)



(b)



(c)

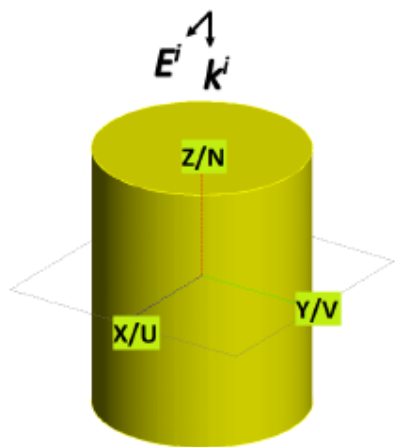
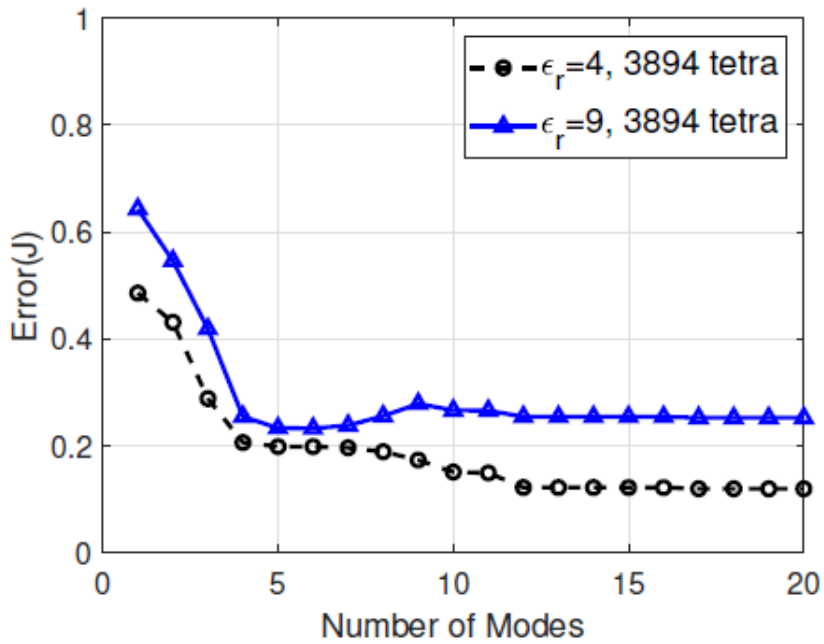
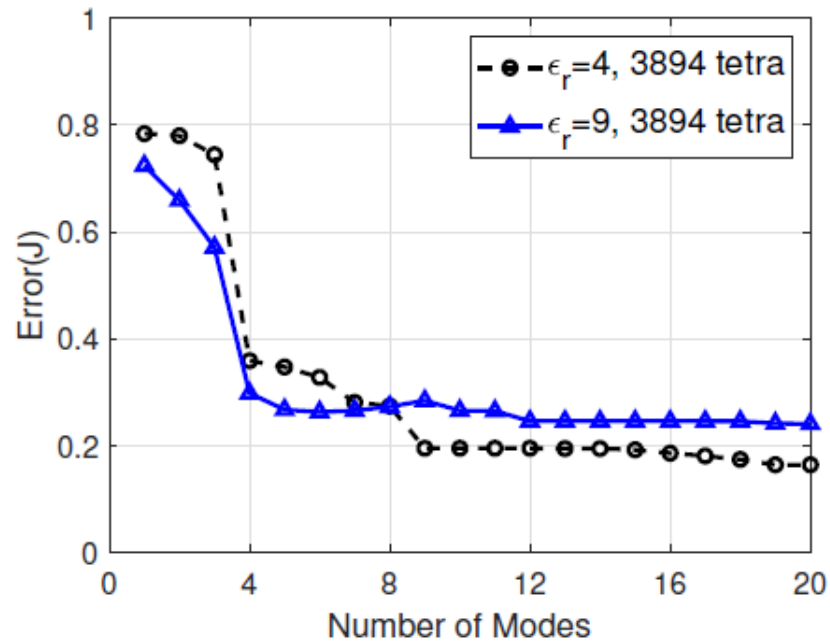


Figure 3: Power ratios of P_{pulse} and P_{SWG} for a scattering problem from a cylinder, $\epsilon_r = 4$, $r = 0.1\lambda_0$; $h = 0.25\lambda_0$, 3885 tetrahedrons, (a) $f = 0.5$ GHz, (b) $f = 0.75$ MHz, (c) $f = 1$ GHz.

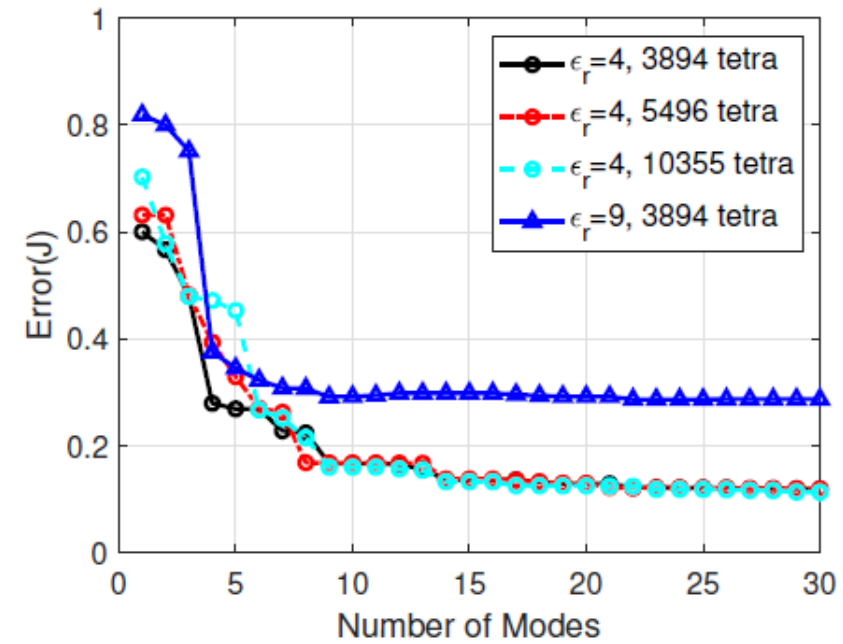
- The power ratios of real and imaginary parts of total power calculated by the SWG and pulse function methods are near unity for 9, 12, and 15 modes at the frequencies $f = 0.5, 0.75,$ and 1 GHz, respectively
- The ratio for the imaginary parts of total power does not deviate from unity



(a)



(b)



(c)

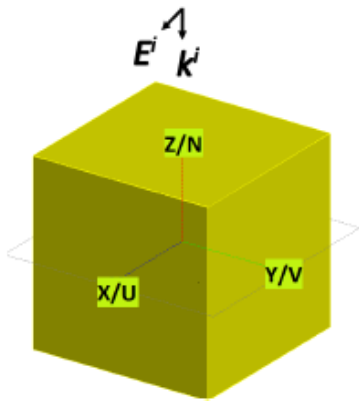


Figure 4: Error between J_{pulse} and J_{SWG} , real part and imaginary parts of J_{pulse} and J_{SWG} involving a scattering problem from a cube, respectively, $\epsilon_r = 4$ and $\epsilon_r = 9$, $\ell_0 = 0.2\lambda_0$, (a) $f = 0.5$ GHz, (b) $f = 0.75$ GHz, (c) $f = 1$ GHz.

- Error(\mathbf{J}) is with $\varepsilon_r = 9$ higher than $\varepsilon_r = 4$ in general with the same number of meshes because of higher λ_{eff}
- Increasing the number of meshes up to 10355 tetrahedrons (TEL= $\lambda_{eff}/20$ for $\varepsilon_r = 4$) does not decrease the error because of small contributions from CMs with large eigenvalues (i.e., non-significant modes)
- Further reduction of this error values will be possible by utilizing higher quadrature rules for test functions and careful singularity treatment
- The error between \mathbf{J}_{pulse} and \mathbf{J}_{SWG} was observed to be decreasing when more eigenvalues are used for the calculation of \mathbf{J}

Conclusion

- Pulse functions and point matching method in VIE
- Easy to solve
- Feasible for CMs extraction of dielectric bodies

THANK YOU